J Comput Electron (2007) 6:321–324
DOI 10.1007/s10825-006-0113-7

Dissipative transport in CNTFETs

Mahdi Pourfath · Hans Kosina · Siegfried Selberherr

Published online: 26 January 2007

Abstract Based on the non-equilibrium Green's function formalism the performance of carbon nanotube field-effect transistors has been studied. The effects of elastic scattering and the impact of parameters of inelastic scattering, such as electron-phonon coupling strength and phonon energy, on the device performance are analyzed.

Keywords Electron-phonon interaction · Non-equilibrium Green's function · Dissipative transport · Carbon nanotube transistors

1 Introduction

A carbon nanotube (CNT) can be viewed as a rolled-up sheet of graphite with a diameter of a few nanometers. Depending on the chiral angle the CNT can be either metallic or semiconducting. Semiconducting CNTs can be used as channels for field-effect transistors (FETs). CNTFETs have been studied in recent years as potential alternatives to CMOS devices because of their capability of ballistic transport [1].

Depending on the work function difference between the metal contact and the CNT, carriers at the metal-CNT interface encounter different barrier heights. Fabrication of devices with positive (Schottky type) [2, 3] and zero (ohmic) [4] barrier heights have been reported. Devices with positive barrier heights have lower on-current and also suffer from ambipolar behavior [5–7], while devices with zero barrier height theoretically [8] and experimentally [1] show better performance. In this work we focus on devices with zero barrier height for electrons. The barrier height for holes is given by the band gap of the CNT.

The non-equilibrium Green's function (NEGF) formalism has been successfully used to investigate the characteristics of nano-meter silicon transistors [9], carbon nanotube based transistors [8, 10], and molecular devices [11]. In this work the NEGF formalism is used to investigate the effect of electron-phonon interaction on the static and dynamic response of CNTFETs.

M. Pourfath (✉) · H. Kosina · S. Selberherr
Institute for Microelectronics, TU Wien,
Gußhausstraße 27–29/E360, 1040 Wien, Austria
e-mail: pourfath@iue.tuwien.ac.at

2 Approach

Due to quantum confinement along the tube circumference, the wave functions of carriers are bound around the CNT and can propagate along the tube axis. Assuming that the potential profile does not vary around the circumference of the CNT, sub-bands can be decoupled [9]. In this work we assume bias conditions in which the first sub-band contributes mostly to the total current. In the mode-space approach [9] the transport equations for each sub-band can be written as [12]:

$$G^{\mathrm{R}}_{\mathbf{r},\mathbf{r}'}(E) = \left[E I - H_{\mathbf{r},\mathbf{r}'}(E) - \Sigma^{\mathrm{R}}_{\mathbf{r},\mathbf{r}'}(E)\right]^{-1} \tag{1}$$

$$G^{<,>}_{\mathbf{r},\mathbf{r}'}(E) = G^{\mathrm{R}}_{\mathbf{r},\mathbf{r}'}(E)\Sigma^{<,>}_{\mathbf{r},\mathbf{r}'}(E)\left[G^{\mathrm{R}}_{\mathbf{r},\mathbf{r}'}(E)\right]^{\dagger} \tag{2}$$

We consider the self-energies due to contacts and electron-phonon interaction, $\Sigma = \Sigma_{\mathrm{s}} + \Sigma_{\mathrm{d}} + \Sigma_{\mathrm{e-ph}}$. The self-energy due to the coupling of the device to the source and drain contacts is only non-zero at the boundaries. In (1) an effective mass Hamiltonian is used. All our calculations assume a CNT with a diameter of $d_{\mathrm{CNT}} = 1.6$ nm corresponding to a bandgap of $E_{\mathrm{G}} = 0.6$ eV. A recursive Green's function method is used for solving (1) and (2).

The self-energy due to electron-phonon interaction comprises contributions of elastic and inelastic scattering mechanisms $\Sigma^{<,>}_{\mathrm{e-ph}} = \Sigma^{<,>}_{\mathrm{el}} + \Sigma^{<,>}_{\mathrm{inel}}$. Assuming local scattering ($\Sigma_{\mathbf{r},\mathbf{r}'} = 0$ for $\mathbf{r} \neq \mathbf{r}'$) the self-energies due to electron-phonon interaction for a single sub-band are given by:

$$\Sigma^{<,>}_{\mathrm{el},(\mathbf{r},\mathbf{r})}(E) = D_{\mathrm{el}} G^{<,>}_{\mathbf{r},\mathbf{r}}(E) \tag{3}$$

$$\Sigma^{<}_{\mathrm{inel},(\mathbf{r},\mathbf{r})}(E) = \sum_{\nu} D^{\nu}_{\mathrm{inel}} [(n_B(\hbar\omega_\nu) + 1) G^{<}_{\mathbf{r},\mathbf{r}}(E + \hbar\omega_\nu) + n_B(\hbar\omega_\nu) G^{<}_{\mathbf{r},\mathbf{r}}(E - \hbar\omega_\nu)] \tag{4}$$

$$\Sigma^{>}_{\mathrm{inel},(\mathbf{r},\mathbf{r})}(E) = \sum_{\nu} D^{\nu}_{\mathrm{inel}} [(n_B(\hbar\omega_\nu) + 1) G^{>}_{\mathbf{r},\mathbf{r}}(E - \hbar\omega_\nu) + n_B(\hbar\omega_\nu) G^{>}_{\mathbf{r},\mathbf{r}}(E + \hbar\omega_\nu)] \tag{5}$$

$$\Im m\big[\Sigma^{\mathrm{R}}_{\mathrm{e-ph},(\mathbf{r},\mathbf{r})}(E)\big] = \frac{1}{2i}[\Sigma^{>}_{\mathrm{e-ph},(\mathbf{r},\mathbf{r})} - \Sigma^{<}_{\mathrm{e-ph},(\mathbf{r},\mathbf{r})}] \tag{6}$$

$$\Re e\big[\Sigma^{\mathrm{R}}_{\mathrm{e-ph},(\mathbf{r},\mathbf{r})}(E)\big] = \frac{1}{\pi}\mathbf{P}\int \frac{\Im m[\Sigma^{\mathrm{R}}_{\mathrm{e-ph},(\mathbf{r},\mathbf{r})}(E')]}{E' - E} dE' \tag{7}$$

where **P** stands for principal part of the integral and ν is the phonon mode. Phonon occupation number, n_{B}, is given by the Bose-Einstein distribution function:

$$n_{\mathrm{B}}(\hbar\omega_\nu) = \frac{1}{\exp(\hbar\omega_\nu / k_{\mathrm{B}}T) - 1} \tag{8}$$

The electron-phonon coupling constant (D) and phonon energy ($\hbar\omega_\nu$) depend on the chirality and the diameter of the CNT [13]. The self-energy is added to the Hamiltonian. The imaginary part of the self-energy (6) broadens the density of states and the real part of the self-energy (7) shifts the density of states. Even for strong electron-phonon coupling the real part is about several 10 meV (Fig. 1.), which is negligible compared to the electrostatic potential.

The transport equations are iterated to achieve convergence of the electron-phonon self-energies, resulting in a self-consistent Born approximation.

The carrier concentration and the current density at some point **r** of the device can be calculated as (9) and (10).

$$n_{\mathbf{r}} = -4i \int G^{<}_{\mathbf{r},\mathbf{r}}(E) \frac{dE}{2\pi} \tag{9}$$

$$j_{\mathbf{r}} = \frac{4q}{\hbar} \int \mathrm{Tr}\big[\Sigma^{<}_{\mathbf{r},\mathbf{r}} G^{>}_{\mathbf{r},\mathbf{r}}(E) - \Sigma^{>}_{\mathbf{r},\mathbf{r}} G^{<}_{\mathbf{r},\mathbf{r}}(E)\big] \frac{dE}{2\pi} \tag{10}$$

The factor 4 in (9) and (10) originates from double spin and double band degeneracy. Carriers are treated as a sheet charge distributed over the surface of the CNT. After convergence of the scattering self energies, the coupled system of transport and Poisson equations is solved iteratively. Details are presented in [14].

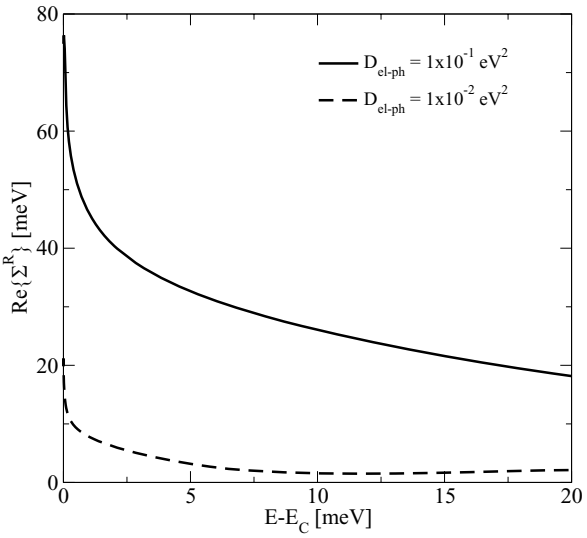

Fig. 1 The real part of $\Sigma^{R}_{\mathrm{e-ph}}$ versus energy for elastic scattering with the band-edge of the conduction band as the reference. Even for strong electron-phonon coupling this term is about several 10 meV, which is negligible compared to the electrostatic potential

3 The effect of electron-phonon interaction

In this section the effects of the electron-phonon coupling strength and the phonon energy on the static and dynamic response of CNTFETs are investigated.

3.1 Static response

With increasing $D_{\mathrm{el-ph}}$ the imaginary part of the self-energy (6) increases, which adds dissipation to the Hamiltonian, and as a result the total current decreases. Figure 2 shows the ratio

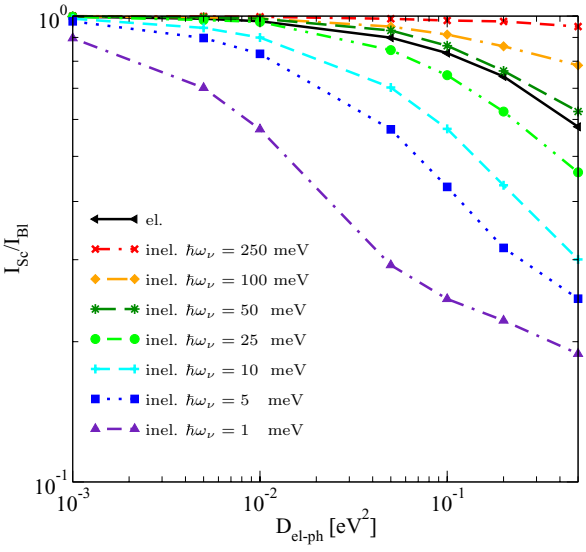

Fig. 2 The ratio of the current with scattering (I_{Sc}) and without scattering (I_{Bl}) versus the strength of electron-phonon coupling ($D_{\mathrm{el-ph}}$) for elastic and inelastic scattering. The length of the CNT is 50 nm

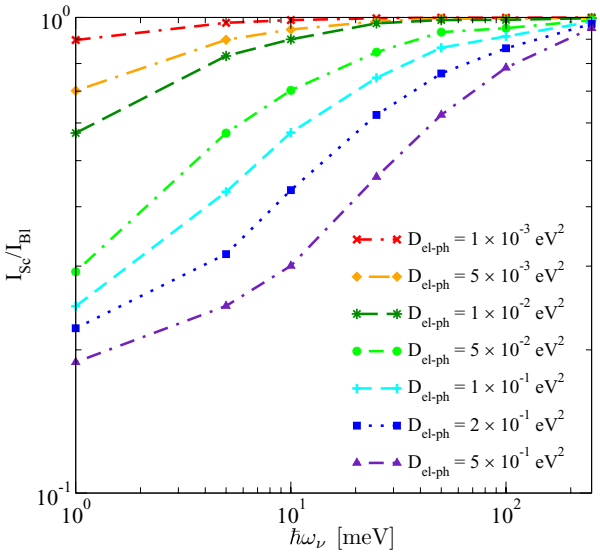

Fig. 3 The ratio of the current with scattering and without scattering versus the phonon energy ($\hbar\omega_\nu$) for inelastic scattering. The length of the CNT is 50 nm

of the current versus $D_{\mathrm{el-ph}}$ with and without scattering (ballistic). Elastic scattering conserves the energy of carriers as in the ballistic case, but the current decreases due to elastic back-scattering of carriers. On the other side, with inelastic scattering the energy of carriers is not conserved. Carriers which acquire enough kinetic energy can emit phonons and scatter into lower energy states. With the increase of phonon energy the current is less reduced, since scattered carriers lose more kinetic energy and the probability for back-scattering decreases [15]. As the phonon energy increases the occupation number (8) decreases exponentially. Therefore, the self-energy decreases and the current is weakly affected even for strong electron-phonon coupling, see Fig. 3. These results are for a device of 50 nm length. Assuming that the ballisticity is inversely proportional to the CNT length, our results is valid for CNTs with a length of less than several hundred nanometers.

3.2 Dynamic response

To investigate the dynamic response of the device we consider the device delay time defined as:

$$\tau = \frac{C_{\mathrm{G}} V_{\mathrm{DD}}}{I_{\mathrm{on}}} \tag{11}$$

Here, $C_{\mathrm{G}}^{-1} = C_{\mathrm{Ins}}^{-1} + C_{\mathrm{Q}}^{-1}$. The quantum capacitance is given by $C_{\mathrm{Q}} = 8\mathrm{q}^2/\mathrm{h}\nu_{\mathrm{F}} \approx 400\mathrm{aF}/\mu\mathrm{m}$, including the twofold band and spin degeneracy [16]. We assume the quantum capacitance limit, where $C_{\mathrm{Q}} \ll C_{\mathrm{Ins}}$.

The device delay time versus the $I_{\mathrm{on}}/I_{\mathrm{off}}$ ratio can be used to compare devices with different geometries and material properties [17]. Figure 4 compares the device delay time

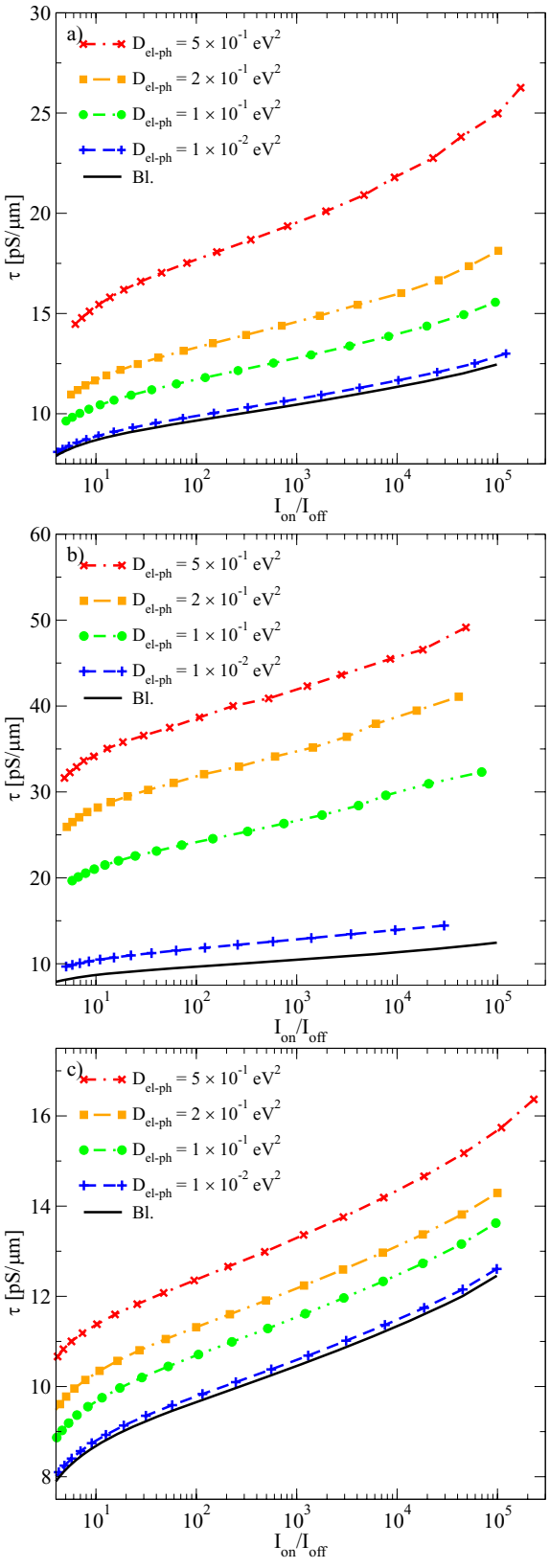

Fig. 4 The effect of electron-phonon interaction on the device delay time versus the $I_{\mathrm{on}}/I_{\mathrm{off}}$ ratio for (a) elastic scattering, (b) inelastic scattering with $\hbar\omega_\nu = 5$ meV, and (c) inelastic scattering with $\hbar\omega_\nu = 100$ meV

versus the I_{on}/I_{off} ratio with and without scattering. Similar to the static response, with increasing electron-phonon coupling the device delay time increases considerably. In the case of inelastic scattering with high energy phonons the device performance is weakly affected.

4 Discussions

In general electron-phonon interaction parameters depends on the diameter and the chirality of the CNT. The calculation of these parameters is presented in [13]. In CNTs the band gap is inversely proportional to the diameter. A rough estimate is $E_G = 0.8\ \text{eV}/d_{CNT}\ \text{nm}$. CNTs with a diameter $d_{CNT} > 2$ nm have a band gap $E_G < 0.4$ eV, which render them unsuitable as channel for FETs. However, the fabrication of devices with a diameter $d_{CNT} < 1$ nm is very difficult. As a result, we limit our study to zigzag CNTs with diameters in the range d_{CNT} =1–2 nm.

In CNTs elastic scattering is caused by acoustic phonons and inelastic scattering occurs due to zone boundary (ZB), optical (OP), and radial breathing (RBM) phonon modes. Considering the class of CNTs we discussed above, the energies of the these phonon modes are $\hbar\omega_{ZB} \approx 160$ and 180 meV, $\hbar\omega_{OP} \approx 200$ meV, and $\hbar\omega_{RBM} \approx 30$ meV respectively [18, 19]. The corresponding coupling coefficients are $D_{inel}^{ZB} \approx 10^{-4}$ and $50 \times 10^{-3}\ \text{eV}^2$, $D_{inel}^{OP} \approx 40 \times 10^{-3}\ \text{eV}^2$, and $D_{inel}^{RBM} \approx 10^{-3}\ \text{eV}^2$ [13, 19]. As discussed in the previous section, for short devices (less than some hundred nano-meter) high energy phonons, such as OP and ZB phonon modes, degrade the performance only weakly, whereas the RBM phonon mode can have a detrimental effect. However, due to weak electron-phonon coupling the RBM mode has a negligible effect at room temperature. The electron-phonon coupling is also weak for acoustic phonon (AP) modes ($D_{el}^{AP} < 10^{-3}\ \text{eV}^2$), which implies weak elastic backscattering of carriers. Therefore, CNTFETs shorter than several hundred nanometers can operate close to the ballistic limit [1].

5 Conclusions

Based on the NEGF formalism we investigated the effect of electron-phonon interaction on the performance of CNTFETs. For elastic scattering, the electron-phonon coupling strength plays an important role. For inelastic scatterin not only the coupling strength, but also the phonon energy is an important parameter. In CNTs either the electron-phonon coupling is weak or the phonon energies are high. Therefore, the performance of short devices is only weakly affected.

Acknowledgment This work has been partly supported by the Austrian Science Fund, contract I79-N16, and the national program for tera-level nano-devices of the Korean ministry of science and technology.

References

1. Javey, A et al.: Self-aligned ballistic molecular transistors and electrically parallel nanotube arrays. Nano Lett. **4**(7), 1319 (2004)
2. Appenzeller, J et al.: Tunneling versus thermionic emission in one-dimensional semiconductors. Phys. Rev. Lett. **92**, 048301 (2004)
3. Heinze, S et al.: Carbon nanotubes as Schottky barrier transistors. Phys. Rev. Lett. **89**, 106801 (2002)
4. Javey, A et al.: Ballistic carbon nanotube field-effect transistors. Lett. Nature **424**(6949), 654 (2003)
5. Pourfath, M et al.: Separated carrier injection control in carbon nanotube field-effect transistors. J. Appl. Phys. **97**, 1061031 (2005)
6. Pourfath, M et al.: Improving the ambipolar behavior of Schottky barrier carbon nanotube field effect transistors. In: Proc. ESSDERC 429–432 (2004)
7. Martel, R et al.: Ambipolar electrical transport in semiconducting single-wall carbon nanotubes. Phys. Rev. Lett. **87**, 256805 (2001)
8. Guo, J et al.: A numerical study of scaling issues for Schottky barrier carbon nanotube transistors. IEEE Trans. Electron Devices **51**(2), 172 (2004)
9. Venugopal, R et al.: Simulating quantum transport in nanoscale transistors: real versus mode-space approaches. J. Appl. Phys. **92**(7), 3730 (2002)
10. Svizhenko, A., Anantram, M.: Effect of scattering and contacts on current and electrostatics in carbon nanotubes. Phys. Rev. B **72**, 085430 (2005)
11. Tian, W et al.: Conductance spectra of molecular wires. J. Chem. Phys **109**(7), 2874 (1998)
12. Datta, S.: Electronic Transport in Mesoscopic Systems. Cambridge University Press (1995)
13. Mahan, G.: Electron-optical phonon interaction in carbon nanotubes. Phys. Rev. B **68**, 125409 (2003)
14. Pourfath, M., Kosina, H.: Fast convergent Schrödinger-Poisson solver for the static and dynamic analysis of carbon nanotube field effect transistors. Lecture Notes in Computer Science **3743**, 578 (2006)
15. Guo, J., Lundstrom, M.: Role of phonon scattering in carbon nanotube field-effect transistors. Appl. Phys. Lett. **86**, 193103 (2005)
16. John, D et al.: Quantum capacitance in nanoscale device modeling. J. Appl. Phys. **96**(9), 5180 (2004)
17. Guo, J et al.: Performance analysis and design optimization of near ballistic carbon nanotube field-effect transistors. In: IEDM Tech. Dig. pp. 703–706 (2004)
18. Park, J et al.: Electron-phonon scattering in metallic single-walled carbon nanotubes. Nano Lett. **4**(3), 517 (2004)
19. Koswatta, S. et al.: Ballisticity of nanotube FETs: role of phonon energy and gate bias. Cond-mat/0511723 (2005)